

A new modified scheme for linear shallow-water equations with distant propagation of irregular wave trains tsunami dispersion type for inviscid and weakly viscous fluids

A.Boussaha^a, A. Laouar^a, A.Guerziz^b, Hossam S.Hassan^{c,*}

^a*Department of Mathematics, Faculty of Sciences, Badji Mokhtar University, P.O. Box 12, 23000 Annaba, Algeria*

^b*Department of Physics, Faculty of Sciences, Badji Mokhtar University, P.O. Box 12, 23000 Annaba, Algeria*

^c*Department of Basic and Applied Science, College of Engineering and Technology, Arab Academy for Science, Technology and Maritime Transport, P.O.BOX 1029 Alexandria, Egypt*

* *Corresponding author, Tel.: +201113334393; fax: +2035622388.*

E-mail addresses: hossams@aast.edu (Hossam S.Hassan), boussahaaicha@yahoo.fr (A. Boussaha), laouar.abdelhamid@univ-annaba.org (A. Laouar), allaoua.guerziz@univ-annaba.org (A. Guerziz)

Abstract

In this work, we propose a modified scheme for simulating irregular wave trains (IWTs) propagation dispersive of tsunami with suitable initial and boundary conditions by applying the alternating direction implicit (ADI) method. The convergence, stability and consistency criteria of the scheme have been studied. We introduce a weakly dissipative terms into improved linear Boussinesq equations (ILBqs) that permits the mathematical tool to simulating a transoceanic propagation dispersive of tsunami in both ocean and laboratory experimental. The new numerical dispersion of the proposed model is manipulated to replace the physical dispersion of (ILBqs) by controlling dispersion-correction parameters. The new model developed in this study is applied to propagation of Heraklion tsunami scenario1(HTS1)of the 365 AD earthquake. The resulting scheme is efficient and practical to implement. Furthermore, a comparison between the present results with another existing numerical method has been reported and we found that they are in a good agreement.

Keywords: Improved Linear Boussinesq equations; Numerical dispersion-correction parameter; ADI scheme; Dissipation effects; Tsunamis

Nomenclature

B Pure curve fitting parameter

BW Bichromatic Wave

c Phase velocity of a linear shallow-water wave

C_r Courant number

g Gravity acceleration

h Still-water depth

I Identity matrix

M, N Depth-average volume fluxes in the x – and y –axis directions

M_0, N_0 Initial value of M and N

t Time

Greek Symbols

$\alpha_1, \alpha_2, \alpha_3$ Dispersion-correction factors

η Free surface displacement

η_0 Initial value of η

$\eta_{\frac{1}{10}}, \eta_{\frac{1}{100}}$ Numerical solutions of the free surface displacement at $\Delta x = \frac{1}{10}, \frac{1}{100}$

ν Kinematic viscosity (Constant)

$\rho^{\Delta t}$ Amplification factor

λ_x Sub-interval number which discretize x –interval

λ_y Sub-interval number which discretize y –interval

$\Delta x, \Delta y$ Spatial grid sizes

Δt Time step size

$\delta \cdot$ Derivative operator

Abbreviations

ADI Alternating direction implicit

CLBqs Classical linear Boussinesq equations

CPU Computational process uniform

HTS1 Heraklion tsunami scenario 1

ILBqs Improved linear Boussinesq equations

IWTs Simulating irregular wave trains

LSWqs Linear shallow-water equations

PC Predictor Corrector

Subscripts

i, j Spatial nodes in x –and y –axis directions

Superscripts

k Time level

1. Introduction

The first model for the propagation of surface waves over shallow inviscid fluid layer is Boussinesq's equation. A perturbation method to solve the Laplace equation in the bulk is developed by Boussinesq [1-2]. He arrived at a generalized wave equation that contains dispersion in addition to the standard terms, [3].

Analytical and numerical studies with improved characteristics of the Boussinesq models have received considerable attention of scientists. Daripa and Hua [4] considered an ill-posed Boussinesq equation which arises in shallow water waves and nonlinear lattices. They used a finite difference scheme to investigate the effect of the short-wave instability on the numerical accuracy of the exact solitary wave solution of the equation in order to develop numerical techniques for constructing good approximate solutions. They presented a computational evidence which indicates that numerical accuracy of the solutions is lost very quickly due to severe growth of numerical errors, round off as well as truncation. Filtering and regularization techniques are used to control growth of these errors and to provide better approximate solutions of the equation.

Bratsos et al. [5] applied two different linearized schemes to the parametric finite-difference scheme concerning the numerical solution of the Boussinesq equation. The nonlinear term of the equation is substituted by an appropriate value at the first linearized scheme. They used Taylor's expansion at the second scheme. For local truncation error, stability and convergence, both schemes are analyzed. They examined the results of the experiments for their accuracy for the single and the double-soliton waves to known from the bibliography numerical schemes.

Antonopoulos et al. [6] considered the one-parameter family of Bona-Smith systems, which belongs to the class of Boussinesq systems modelling two-way propagation of long waves of small amplitude on the surface of water in a channel. They studied numerically three initial-boundary value problems for these systems corresponding to homogeneous Dirichlet, reflection, and periodic boundary conditions posed at the endpoints of a finite spatial interval. The standard Galerkin-finite element method for the spatial discretization and a fourth-order explicit Runge-Kutta scheme for the time stepping, and analyze the convergence of the fully discrete schemes are used to approximate these problems.

Mitsotakis [7] applied the standard Galerkin-finite element method to the simplified Boussinesq model of surface water wave theory over a variable bottom with homogeneous Dirichlet boundary conditions. They studied the generation and propagation of tsunami waves. The tsunami waves generated by Boussinesq model are compared by the linearized Euler equations. They studied tsunami wave propagation in the case of the Java 2006 event, comparing the results of the Boussinesq model with those produced by the finite-difference code MOST, that solves the shallow water wave equations.

Dougalis et al. [8] considered a three-parameter family of Boussinesq type systems in two space dimensions. The three-dimensional Euler equations are approximated by these systems, and consist of three nonlinear dispersive wave equations that describe two-way propagation of long surface waves of small

amplitude in ideal fluids over a horizontal bottom. They applied Galerkin-finite element method to discretize a class of these systems and error estimates are proved for the resulting continuous time semi-discretizations.

Antonopoulos and Dougalis [9] considered the classical Boussinesq system of water wave theory, which belongs to the class of Boussinesq systems modeling two-way propagation of long waves of small amplitude on the surface of water in a horizontal channel. The initial-boundary-value problem for these systems, corresponding to homogeneous Dirichlet boundary conditions on the velocity variable at the endpoints of a finite interval is discretized, using fully discrete Galerkin-finite element methods of high accuracy. They used the numerical schemes as exploratory tools to study the propagation and interactions of solitary-wave solutions of these systems, as well as other properties of their solutions.

Dutykh and Goubet [10] combined the visco-potential approach with Dirichlet-to-Neumann operator formulation of the water wave problem which can be successfully used for water wave modeling purposes. A long wave model of Boussinesq type is derived by using this novel visco-potential formulation and an asymptotic expansion of the Dirichlet-to-Neumann operator. They also derived the dissipative Boussinesq equations.

The Boussinesq numerical models require a small mesh size to suppress numerical dispersion errors, [11-12]. This consumes huge amounts of computer resources due to the implicit nature of the solution technique to deal with dispersion terms. Thus, the Boussinesq model is not preferred for the simulation of the far-field tsunamis, and linear shallow-water equations (LSWqs) are generally employed instead. Numerical models based on (LSWqs) will suffer from a lack of accuracy. In order to improve that model, we will propose a new numerical scheme in this work.

The effects of frequency dispersion are accumulative and become increasingly important as tsunamis travel a long distance, [13]. The dissipation is an important mathematical concept in both theoretical and experimental physics.

Many tsunamis have highly (IWTs) patterns. Some of them have a high initial peak, followed by successively smaller wave crests and this is related to the nature of the triggering mechanism that formed the wave train, [14]. This phenomenon is called dispersion. For example, a splash induced by an earthquake in ocean, [15]. Consequently, (IWTs) have become interest topical themes research in laboratories worldwide.

The classical linear Boussinesq equations (CLBqs) including the Coriolis force describe the propagation of distant tsunami are given by

$$\frac{\partial \eta}{\partial t} + \frac{\partial M}{\partial x} + \frac{\partial N}{\partial y} = 0, \quad (1.1)$$

$$\frac{\partial M}{\partial t} + gh \frac{\partial \eta}{\partial x} = \frac{h^2}{3} \left(\frac{\partial^3 M}{\partial t \partial x^2} + \frac{\partial^3 N}{\partial t \partial x \partial y} \right), \quad (1.2)$$

$$\frac{\partial N}{\partial t} + gh \frac{\partial \eta}{\partial y} = \frac{h^2}{3} \left(\frac{\partial^3 N}{\partial t \partial y^2} + \frac{\partial^3 M}{\partial t \partial x \partial y} \right), \quad (1.3)$$

where the variables are given in the nomenclature. The right-hand side terms of Eqs. (1.2)- (1.3) represent the frequency dispersion.

Madsen et al. [11] proposed a new form of the (CLBqs) in order to improve their dispersion characteristics. They demonstrated that, the depth-limitation of the new equations is much less restrictive than (CLBqs), and it is possible to simulate the propagation of (IWTs) travelling from deep water to shallow water by introducing the bidimensional****(ILBqs) which given by

$$\frac{\partial \eta}{\partial t} + \frac{\partial M}{\partial x} + \frac{\partial N}{\partial y} = 0, \tag{1.4}$$

$$\frac{\partial M}{\partial t} + gh \frac{\partial \eta}{\partial x} = h^2 \left(B + \frac{1}{3} \right) \left(\frac{\partial^3 M}{\partial t \partial x^2} + \frac{\partial^3 N}{\partial t \partial x \partial y} \right) + Bgh^3 \left(\frac{\partial^3 \eta}{\partial x^3} + \frac{\partial^3 \eta}{\partial x \partial y^2} \right), \tag{1.5}$$

$$\frac{\partial N}{\partial t} + gh \frac{\partial \eta}{\partial y} = h^2 \left(B + \frac{1}{3} \right) \left(\frac{\partial^3 N}{\partial t \partial y^2} + \frac{\partial^3 M}{\partial t \partial x \partial y} \right) + Bgh^3 \left(\frac{\partial^3 \eta}{\partial y^3} + \frac{\partial^3 \eta}{\partial x^2 \partial y} \right). \tag{1.6}$$

Substitution from (1.5)- (1.6) into (1.4) and eliminate M and N, yields

$$\frac{\partial^2 \eta}{\partial t^2} - gh \left(\frac{\partial^2 \eta}{\partial x^2} + \frac{\partial^2 \eta}{\partial y^2} \right) = -Bgh^3 \left(\frac{\partial^4 \eta}{\partial x^4} + 2 \frac{\partial^4 \eta}{\partial y^2 \partial x^2} + \frac{\partial^4 \eta}{\partial y^4} \right) + h^2 \left(B + \frac{1}{3} \right) \left(\frac{\partial^4 \eta}{\partial t^2 \partial x^2} + \frac{\partial^4 \eta}{\partial t^2 \partial y^2} \right). \tag{1.7}$$

Eq.(1.7) is called (ILBq). The frequency dispersion given by the right-hand side terms of Eq.(1.7) may cause serious numerical difficulty in practice because of higher order derivatives. An alternative way is to solve a set of lower order partial differential equations, it is the (LSWqs). The numerical dispersion induced by the numerical scheme can be manipulated to represent the physical frequency dispersion of the (ILBq).

In this study, weakly dissipative terms are introduced into (LSWqs) modified system. We employ the third-order ADI predictor corrector (PC) scheme for spatial****derivatives with three-time level. As a result, both numerical weakly dissipation and linear dispersion are kept with good precision. Subsequently, we shall show that even oceanic propagation of dispersive waves can be quite efficiently modeled using mathematically well-founded (LSWqs) modified scheme.***The convergence, stability and consistency criteria of the scheme are also studied. The results are compared with the work of Madsen et al.[11].

2. Mathematical Formulation and Discretization of the Problem

Using transoceanic propagation of (HTS1) well described and realized for the site (35.3635°N, 25.1236°E) in [16]. We require the explicit inclusion of weak dissipative effects, to make the dispersion phenomenon more realistic than the traditional problems whose neglected all effects of the viscosity. Hence, the theory of visco-potential flows [10] has been introduced. In tsunami propagation problems, one can suppose a condition of full reflectivity, which is equivalent to limiting the domain by

means of an infinitely high vertical wall and is useful to handle waves travelling in closed basins and in laboratory tanks, see Figure1. ******In Figure1, l_{beach} represents the region where the artificial damping terms to the kinematic and dynamic free surface boundary condition are added in order to suppress reflections.

The (LSWEs) are given by

$$\frac{\partial \eta}{\partial t} + \frac{\partial M}{\partial x} + \frac{\partial N}{\partial y} = 0, \quad (2.1)$$

$$\frac{\partial M}{\partial t} + gh \frac{\partial \eta}{\partial x} = 0, \quad (2.2)$$

$$\frac{\partial N}{\partial t} + gh \frac{\partial \eta}{\partial y} = 0. \quad (2.3)$$

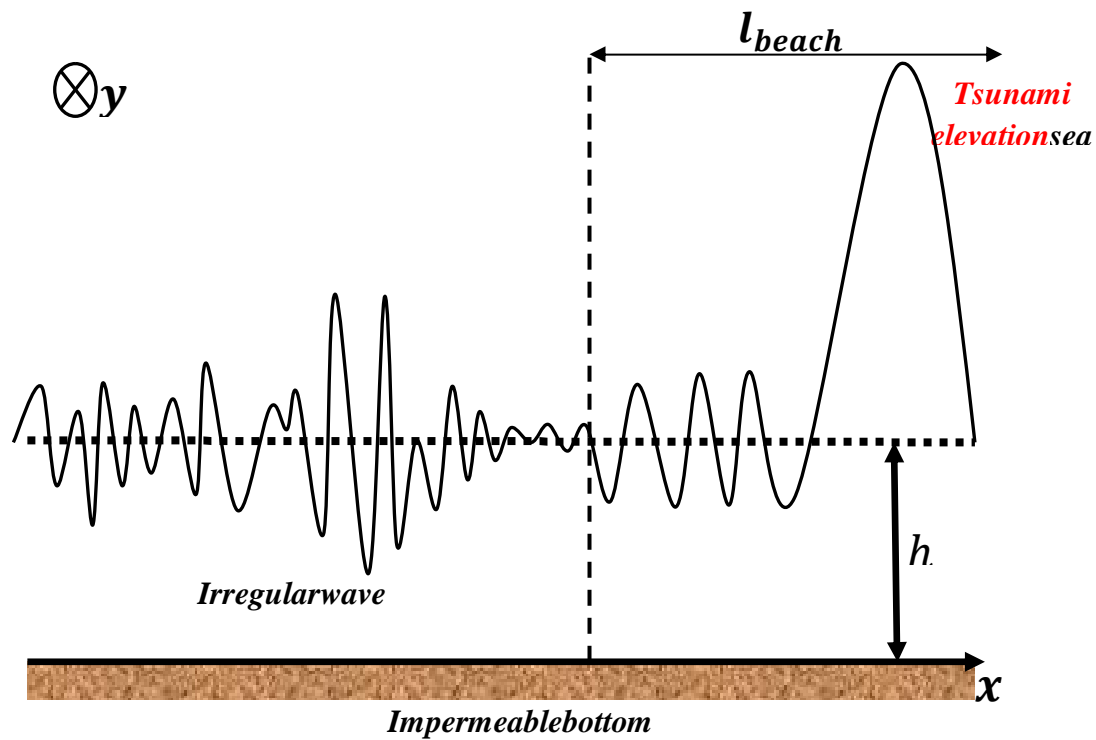


Figure1. Phenomenon description

Using the finite difference method, where the domain is discretized in a regular grid $\lambda_x \times \lambda_y$ with a finite number of nodes spaced Δx and Δy , *********the time axis is discretized in regular steps Δt , and the derivatives are replaced by differences over small intervals. The accuracy of the method depends on the density of points

considered and on the truncation error of the computation. The fluxes M and N are calculated over a grid that is shifted with respect to the grid used to compute by a grid half-step in all the variables, i.e., along x,y and t, respectively, Figure 2. All the quantities can be calculated using the information of the previous time step, identified by the index k, while i and j refer to x and y coordinates, respectively. The numerical computations are performed in the order indicated by the previous equations. At the time step k, firstly, one calculates the discharge fluxes $M_{i+1/2,j}^{k+1/2}$ and $N_{i,j+1/2}^{k+1}$ and then the sea surface elevation $\eta_{i,j}^{k+1}$ by using the values available at the previous time step $\eta_{i,j}^{k+1/2}$ and $\eta_{i,j}^k$.

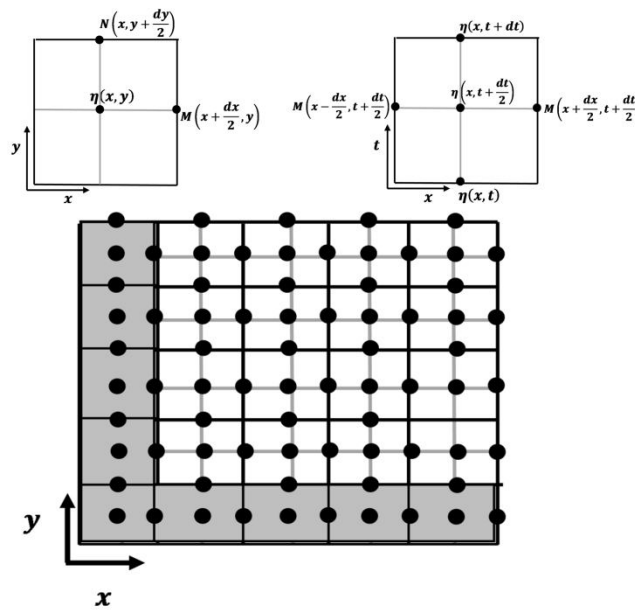


Figure 2. Sketch of the staggered grid technique.

In Figure 2, the left upper panel represents the definition of the discretized variables on a space cell while the right upper panel represents the time axis but restricted to sea surface elevation and the flux in the x direction M. Elevation is computed in the centre of the cell, while fluxes M and N are shifted by a half spatial step along their respective directions. The lower panel is a sample of a grid with grey cells on the bottom and on the left side of the grid. These are ghost cells that are outside the computational domain where only the discharge flux component on the side in common with white cells is computed.

2.1 Dispersion-dissipation Scheme

Now we are going to introduce weak dissipative effects directly into (LSWqs)*** which will be modified to (ILBqs). We put $2\nu \left(\frac{\partial^2 \eta}{\partial x^2} + \frac{\partial^2 \eta}{\partial y^2} \right)$, $\frac{2\nu}{h} \frac{\partial^2 M}{\partial x^2}$ and

$\frac{2\nu}{h} \frac{\partial^2 N}{\partial y^2}$ into Eqs.(1.4)-(1.6), respectively. The new set of equations with the above additional expressions describe a (PDEs) problem that we shall restrict our study to the non-advective term, numerical linear dispersion and weak dissipation terms. The new proposed scheme is given by the following procedure.

The x –sweep equations, in which $\eta_{i,j}^{k+\frac{1}{2}}$ and $M_{i+\frac{1}{2},j}^{k+\frac{1}{2}}$ are the unknown variables:

Predictor stage

$$\begin{aligned} & \frac{\eta_{i,j}^{k+\frac{1}{2}} - \eta_{i,j}^k}{\frac{\Delta t}{2}} + \frac{M_{i+\frac{1}{2},j}^{k+\frac{1}{2}} - M_{i-\frac{1}{2},j}^{k+\frac{1}{2}}}{\Delta x} + \frac{N_{i,j+\frac{1}{2}}^k - N_{i,j-\frac{1}{2}}^k}{\Delta y} \\ & = \frac{2\nu}{(\Delta x)^2} \left(\eta_{i+1,j}^{k+\frac{1}{2}} - 2\eta_{i,j}^{k+\frac{1}{2}} + \eta_{i-1,j}^{k+\frac{1}{2}} + \eta_{i,j+1}^k - 2\eta_{i,j}^k + \eta_{i,j-1}^k \right). \end{aligned} \quad (2.4)$$

Corrector stage

$$\begin{aligned} & \frac{M_{i+\frac{1}{2},j}^{k+\frac{1}{2}} - M_{i+\frac{1}{2},j}^k}{\frac{\Delta t}{2}} + gh \frac{\eta_{i+1,j}^{k+\frac{1}{2}} - \eta_{i,j}^{k+\frac{1}{2}}}{\Delta x} + \frac{\alpha_1}{12\Delta x} gh \left(\eta_{i+2,j}^{k+\frac{1}{2}} - 3\eta_{i+1,j}^{k+\frac{1}{2}} + 3\eta_{i,j}^{k+\frac{1}{2}} - \eta_{i-1,j}^{k+\frac{1}{2}} \right) \\ & + \frac{\alpha_2}{12\Delta x} gh \left[\left(\eta_{i+1,j+1}^{k+\frac{1}{2}} - 2\eta_{i+1,j}^{k+\frac{1}{2}} + \eta_{i+1,j-1}^{k+\frac{1}{2}} \right) - \left(\eta_{i,j+1}^{k+\frac{1}{2}} - 2\eta_{i,j}^{k+\frac{1}{2}} + \eta_{i,j-1}^{k+\frac{1}{2}} \right) \right] \\ & + \frac{\alpha_3}{4\Delta x} gh \left[\left(\eta_{i+1,j}^{k+1} - 2\eta_{i+1,j}^{k+\frac{1}{2}} + \eta_{i+1,j}^k \right) - \left(\eta_{i,j}^{k+1} - 2\eta_{i,j}^{k+\frac{1}{2}} + \eta_{i,j}^k \right) \right] \\ & = \frac{2\nu}{h(\Delta x)^2} \left(M_{i+\frac{3}{2},j}^{k+\frac{1}{2}} - 2M_{i+\frac{1}{2},j}^{k+\frac{1}{2}} + M_{i-\frac{1}{2},j}^{k+\frac{1}{2}} \right). \end{aligned} \quad (2.5)$$

The y –sweep equations, in which $\eta_{i,j}^{k+1}$ and $N_{i,j+\frac{1}{2}}^{k+1}$ ***are the unknown variables:

Predictor stage

$$\begin{aligned} & \frac{\eta_{i,j}^{k+1} - \eta_{i,j}^{k+\frac{1}{2}}}{\frac{\Delta t}{2}} + \frac{M_{i+\frac{1}{2},j}^{k+\frac{1}{2}} - M_{i-\frac{1}{2},j}^{k+\frac{1}{2}}}{\Delta x} + \frac{N_{i,j+\frac{1}{2}}^{k+1} - N_{i,j-\frac{1}{2}}^{k+1}}{\Delta y} \\ &= \frac{2\nu}{(\Delta x)^2} \left(\eta_{i+1,j}^{k+\frac{1}{2}} - 2\eta_{i,j}^{k+\frac{1}{2}} + \eta_{i-1,j}^{k+\frac{1}{2}} + \eta_{i,j+1}^{k+1} - 2\eta_{i,j}^{k+1} + \eta_{i,j-1}^{k+1} \right). \end{aligned} \tag{2.6}$$

Corrector stage

$$\begin{aligned} & \frac{N_{i,j+\frac{1}{2}}^{k+1} - N_{i,j+\frac{1}{2}}^{k+\frac{1}{2}}}{\frac{\Delta t}{2}} + gh \frac{\eta_{i,j+1}^{k+1} - \eta_{i,j}^{k+1}}{\Delta y} + \frac{\alpha_1}{12\Delta y} gh (\eta_{i,j+2}^{k+1} - 3\eta_{i,j+1}^{k+1} + 3\eta_{i,j}^{k+1} - \eta_{i,j-1}^{k+1}) \\ &+ \frac{\alpha_2}{12\Delta y} gh [(\eta_{i+1,j+1}^{k+1} - 2\eta_{i,j+1}^{k+1} + \eta_{i-1,j+1}^{k+1}) - (\eta_{i,j+1}^{k+1} - 2\eta_{i,j}^{k+1} + \eta_{i-1,j}^{k+1})] \\ &+ \frac{\alpha_3}{4\Delta y} gh \left[\left(\eta_{i,j+1}^{k+1} - 2\eta_{i,j+\frac{1}{2}}^{k+\frac{1}{2}} + \eta_{i,j}^k \right) - \left(\eta_{i,j}^{k+1} - 2\eta_{i,j+\frac{1}{2}}^{k+\frac{1}{2}} + \eta_{i,j}^k \right) \right] \\ &= \frac{2\nu}{h(\Delta y)^2} \left(N_{i,j+\frac{3}{2}}^{k+1} - 2N_{i,j+\frac{1}{2}}^{k+1} + N_{i,j-\frac{1}{2}}^{k+1} \right). \end{aligned} \tag{2.7}$$

The values of the dispersion-correction factors α_1, α_2 and α_3 **** will be determined later on. ****To the best of our knowledge, this is the first dissipative (LSW) modified scheme which contains a third order derivative of space at three times level. We can consider the inviscid case as a particular problem of the system of Eqs.(2.4)-(2.7) if ν vanishes, i.e., when we neglect all viscosity effects.

2.1.1 Initial and Boundary Conditions

In case of a tsunami induced by an earthquake, the initial conditions assigned for $t = 0$ are expressed by $\eta(x, y, 0) = \eta_0(x, y) = -h$ and $M(x, y, 0) = N(x, y, 0) = 0$. In terms of discretized variables, it can be written as $M_{i,j}^0 = N_{i,j}^0 = N_{i,j}^{1/2} = 0, \eta_{i,j}^0 = \eta_0(x_i, y_j) = -h$. At the boundaries of the computational domain, it is required to set conditions prescribing specific behaviour for the wave fields. In the actual model, boundary conditions are applied to the discharged fluxes in the nodes that are placed in the right (east) and the upper (north) sides of the boundary cells. Instead, all the

cells of the last column, i.e., cells $(\lambda_x, j; j = 1, 2, \dots, \lambda_y)$, are an integral part of the domain, and their right sides constitute the right side of the grid.

The boundary conditions for the considered grid can be given through the following formulas:

- (i) $M_{1+1/2,j}^{k+1/2} = 0$, vertical wall on the left side,
 - (ii) $M_{\lambda_x+1/2,j}^{k+1/2} = 0$, vertical wall on the right side,
 - (iii) $M_{1+1/2,j}^{k+1/2} = \frac{1}{\Delta x} [(\Delta x - c \Delta t)M_{1+1/2,j}^k + c \Delta t M_{2+1/2,j}^k]$, open on the left side,
 - (iv) $M_{\lambda_x+1/2,j}^{k+1/2} = \frac{1}{\Delta x} [(\Delta x - c \Delta t)M_{\lambda_x+1/2,j}^k + c \Delta t M_{\lambda_x-1/2,j}^k]$, open on the right side,
- (2.8)

where,

$$c = \sqrt{gh}. \tag{2.9}$$

Analogous conditions can be imposed on the lower and upper boundary of the mesh involving the y component of the flux N. The Eqs. (2.4)-(2.7) can be easily generalized to domains of arbitrary shape. If the grid considered before contains a basin covered only by a subset of the grid cells, and if the right side of cell (i, j) happens to form part of the left boundary of the basin, i.e. the cell (i, j) does not belong to the basin, but the cell $(i + 1, j)$ belongs, hence the boundary conditions (2.8) can be re-written as

$$M_{i+1/2,j}^{k+1/2} = 0, \text{ vertical wall on the left side,} \tag{2.10}$$

$$M_{i+1/2,j}^{k+1/2} = \frac{1}{\Delta x} [(\Delta x - c \Delta t)M_{i+1/2,j}^k + c \Delta t M_{i+3/2,j}^k], \text{ open on the left side.} \tag{2.11}$$

2.2 Determination of Dispersion-correction Parameters

Following the approach suggested by Warming and Hyett in [17], the Taylor series expansions of the variables η, M and N at the point represented by (k, i, j) are applied to Eqs. (2.4)-(2.7) when v is equal to zero. To derive a resulting modified equation, some higher time derivatives are replaced by the corresponding spatial derivatives and the volume flux components, M and N , are eliminated. After a lengthy algebra, a modified equation for η is obtained as follow:

$$\begin{aligned} &\frac{\partial^2 \eta}{\partial t^2} - c^2 \left(\frac{\partial^2 \eta}{\partial x^2} + \frac{\partial^2 \eta}{\partial y^2} \right) - c^2 \frac{(\Delta x)^2}{12} (1 + \alpha_1 - C_r^2) \left(\frac{\partial^4 \eta}{\partial x^4} + 2 \frac{\partial^4 \eta}{\partial x^2 \partial y^2} + \frac{\partial^4 \eta}{\partial y^4} \right) \\ &\quad + (1 + \alpha_1 - \alpha_2) c^2 \frac{(\Delta x)^2}{6} \frac{\partial^4 \eta}{\partial x^2 \partial y^2} \\ &- c^2 \frac{(\Delta t)^2}{4} (1 - \alpha_3) \left(\frac{\partial^4 \eta}{\partial x^2 \partial t^2} + \frac{\partial^4 \eta}{\partial y^2 \partial t^2} \right) = O((\Delta x)^3, (\Delta x)^2 \Delta t, (\Delta t)^2 \Delta x, (\Delta t)^3), \end{aligned} \tag{2.12}$$

in which a uniform grid is used, i.e. $\Delta x = \Delta y$. The Courant number is given by $C_r = c \Delta t / \Delta x$. The leading order terms in Eq.(2.12) are the same as those in the wave equation. The terms of $O((\Delta x)^2)$ and of higher order are the results of numerical discretization. Comparing Eq.(2.12) with the (ILBq) (1.7), these equations are seen to be identical as long as the following relations are satisfied:

$$\alpha_1 = C_r^2 - \frac{12Bh^2}{(\Delta x)^2} - 1, \tag{2.13}$$

$$\alpha_2 = \alpha_1 + 1, \tag{2.14}$$

And

$$\alpha_3 = 1 - \frac{(B + \frac{1}{3})h^2}{gh(\Delta t)^2}. \tag{2.15}$$

The value of B is not limited to the values discussed in [11]. To verify the stability condition of the current ADI (2.4)-(2.7) scheme, the value of B**** can be chosen as

$$(C_r^2 - 2) \frac{(\Delta x)^2}{12h^2} \leq B \leq \frac{g(\Delta t)^2}{12h}. \tag{2.16}$$

The following relation is obtained if B unique in Eqs. (2.4)-(2.7)

$$(\Delta x)^2 = 4h^2 - 2gh(\Delta t)^2. \tag{2.17}$$

In our study, the spatial grid size Δx and time step size Δt ***** will be determined from Eq.(2.17).

2.3 Existence and uniqueness of the Solution

A mesh of more delicate is considered, taking into account the effects of both numerical linear dispersion and weak dissipation effects. Then, from Eqs.(2.4)-(2.7) we get

$$A_x \eta^{k+\frac{1}{2}} = U_x \eta^k + V_x N^k, \tag{2.18}$$

$$M^{k+\frac{1}{2}} = E_x [Z_x \eta^k + W_x \eta^{k+\frac{1}{2}} + S_x \eta^{k+1}], \tag{2.19}$$

$$N^k = [N_{1,\frac{3}{2}}^k, \dots, N_{\lambda_x,\frac{3}{2}}^k; N_{1,\frac{5}{2}}^k, \dots, N_{\lambda_x,\frac{5}{2}}^k; \dots; N_{1,\lambda_y+\frac{1}{2}}^k, \dots, N_{\lambda_x,\lambda_y+\frac{1}{2}}^k]^T, \tag{2.20}$$

$$M^{k+\frac{1}{2}} = [M_{\frac{3}{2},1}^{k+\frac{1}{2}}, \dots, M_{\frac{3}{2},\lambda_y}^{k+\frac{1}{2}}; M_{\frac{5}{2},1}^{k+\frac{1}{2}}, \dots, M_{\frac{5}{2},\lambda_y}^{k+\frac{1}{2}}; \dots; M_{\lambda_x+\frac{1}{2},1}^{k+\frac{1}{2}}, \dots, M_{\lambda_x+\frac{1}{2},\lambda_y}^{k+\frac{1}{2}}]^T, \tag{2.21}$$

where,

$$\eta^k = [\eta_{1,1}^k, \dots, \eta_{\lambda_x,1}^k; \eta_{1,2}^k, \dots, \eta_{\lambda_x,2}^k; \dots; \eta_{1,\lambda_y}^k, \dots, \eta_{\lambda_x,\lambda_y}^k]^T, \quad (2.22)$$

is applied to iterate $k + 1/2$ and $k + 1$.

In Eqs. (2.18)-(2.19) we can replace i by j , x by y , M by N and vice versa, then we can also replace k by $(k + 1/2)$ and $(k + 1/2)$ by $(k + 1)$. Except we keep the last term of Eq. (2.19) as it is. Like this we get the full matrix form of (2.4)-(2.7) system. All the matrices are presented and described in the Appendix. We use the Gauss-Seidel iterative method because of its high stability with respect to rounding errors. When the terms located on the diagonal of triangular matrix A_x (resp., A_y) are all different from zero, the rank of this matrix is equal to matrix order λ_x (resp., λ_y), so it exists a solution for (2.4)-(2.7) system. **On the other side, the rank is equal to unknown numbers, then the solution of (2.4)-(2.7) system is unique.**

2.4 Convergence of the Scheme

In this section, we shall demonstrate that ADI defined by Eqs (2.4)-(2.7) is stable. By obtaining the local discretization error****and the well-known classical theorem [18], we concluded that,****the scheme is convergent.

2.4.1 Stability Analysis

The solution of****the Eqs. (2.4)-(2.7) can be written in the following Fourier forms,[19]:

$$\eta = \eta_0 \rho^t e^{imx} e^{ily}, \quad (2.23)$$

$$M = M_0 \rho^t e^{imx} e^{ily}, \quad (2.24)$$

$$N = N_0 \rho^t e^{imx} e^{ily}. \quad (2.25)$$

In the stability analysis, the amplification factor, $|\rho^{\Delta t}|$, should be less than or equal to unity.

Substitution****from Eqs.****(2.23)-(2.25) into Eqs.(2.4)-(2.7) and using the notations

$$\begin{aligned} t &= k_0 \Delta t, \quad (k_0 = 0, 1, 2, \dots, k, \dots), \\ x &= i_0 \Delta x, \quad (i_0 = 0, 1, 2, \dots, i, \dots), \\ y &= j^0 \Delta y, \quad (j_0 = 0, 1, 2, \dots, j, \dots), \end{aligned} \quad (2.26)$$

yields the following matrix form of a linear system

$$\begin{bmatrix}
 \frac{2(\frac{\Delta t}{\rho^2}-1)}{(\frac{\Delta t}{\rho^2}+1)} + \frac{4vr_x(\sin^2\theta_x+\sin^2\theta_y)}{h\Delta x} & \hat{r}_x\sin\theta_x & \hat{r}_y\sin\theta_y & \eta_0 \\
 \frac{\hat{r}_x g h \sin\theta_x}{3} \left[\rho^{\frac{\Delta t}{2}}(3-\alpha_1\sin^2\theta_x-\alpha_2\sin^2\theta_y) + 3\alpha_3(\rho^{\Delta t}-2\rho^{\frac{\Delta t}{2}}+1)/4 \right] & (\frac{\Delta t}{\rho^2}-1) + \frac{4vr_x\rho^{\frac{\Delta t}{2}}\sin^2\theta_x}{h\Delta x} & 0 & M_0 \\
 \frac{\hat{r}_y g h \sin\theta_y}{3} \left[\rho^{\frac{\Delta t}{2}}(3-\alpha_1\sin^2\theta_y-\alpha_2\sin^2\theta_x) + 3\alpha_3(\rho^{\Delta t}-2\rho^{\frac{\Delta t}{2}}+1)/4 \right] & 0 & (\frac{\Delta t}{\rho^2}-1) + \frac{4vr_y\rho^{\frac{\Delta t}{2}}\sin^2\theta_y}{h\Delta y} & N_0
 \end{bmatrix} = 0, \tag{2.27}$$

where,

$$r_x = \frac{\Delta t}{\Delta x}, \quad r_y = \frac{\Delta t}{\Delta y}, \quad \theta_x = \frac{m\Delta x}{2} \text{ and } \theta_y = \frac{l\Delta y}{2}.$$

Since the system of linear equations given in matrix form (2.27) is homogeneous, the determinant of the coefficient matrix must vanish to get nontrivial solutions. Assume, $\Delta x = \Delta y$ for simplicity.

For the amplification factor

$$\rho^{\Delta t} = 1, \tag{2.28}$$

The Courant number can be found from

$$C_r = \sqrt{0.25 + \frac{gh(3-\sin^2\theta_x) + (3-\sin^2\theta_y) - \alpha_1(gh+1)(\sin^2\theta_x + \sin^2\theta_y)}{12v^2(\sin^2\theta_x + \sin^2\theta_y)}}. \tag{2.29}$$

In the proposed scheme, the dispersion-correction factor α_1 is ranged from -1 to $(1 + \frac{3v^2}{gh+1})$, to satisfy the stability condition (2.28), while, in the transoceanic propagation, as $h \gg v$, the value of α_1 lies between $-1 \leq \alpha_1 \leq 1$. In (2.29), the largest value of the Courant number is 0.5, when $\sin\theta_x = \sin\theta_y = 1$ at $\alpha_1 = 1$. If the water depth is zero, the dispersion-correction factor $\alpha_1 = -1$, so, the value of the Courant number will be $C_r \leq [0.25 + 1/6v^2]^{0.5}$. Thus, in the real problem, the proposed scheme has the largest allowable Courant number. Then, the dispersion-correction factor α_1 plays an important role in the stability condition. As α_1 increases the largest allowable Courant number decreases.

2.4.2 Consistency of the Numerical Scheme

The intermediate ADI solution introduces an added complication, thus we can either combine separate estimates of the local discretization errors of the predictor and corrector steps, [20].

We can eliminate $\eta_{i,j}^{k+\frac{1}{2}}$ by adding (2.4) and (2.6) in predictor stage. The result is

$$\begin{aligned} \eta_{i,j}^{k+1} - \eta_{i,j}^k &= \left(\frac{v r_x}{\Delta x} \delta_{xx} + \frac{v r_y}{\Delta y} \delta_{yy} \right) (\eta_{i,j}^{k+1} + \eta_{i,j}^k) - \frac{r_x}{2} \delta_x (M_{i,j}^{k+1} + M_{i,j}^k) \\ &\quad - \frac{r_y}{2} \delta_y (N_{i,j}^{k+1} + N_{i,j}^k), \end{aligned} \quad (2.30)$$

where,

$$\begin{aligned} \delta_x &= \eta_{i+\frac{1}{2},j} - \eta_{i-\frac{1}{2},j}, \\ \delta_y &= \eta_{i,j+\frac{1}{2}} - \eta_{i,j-\frac{1}{2}}, \\ \delta_{xx} &= \eta_{i+1,j} - 2\eta_{i,j} + \eta_{i-1,j}, \\ \delta_{yy} &= \eta_{i,j+1} - 2\eta_{i,j} + \eta_{i,j-1}. \end{aligned} \quad (2.31)$$

Dividing by Δt , gathering all terms on the right side, replacing the numerical approximation by any smooth function, and subtracting the result from the differential equation (2.4) or (2.6), yields the local discretization error as

$$\begin{aligned} \Delta t \tau_{i,j}^k &= \Delta t \eta_t + M_x + N_y - v(\eta_{xx} + \eta_{yy}) \Big|_{i,j}^k - \left(1 - \frac{v r_x}{\Delta x} \delta_{xx} - \frac{v r_y}{\Delta y} \delta_{yy} \right) \eta_{i,j}^{k+1} \\ &\quad + \left(1 + \frac{v r_x}{\Delta x} \delta_{xx} + \frac{v r_y}{\Delta y} \delta_{yy} \right) \eta_{i,j}^k - \frac{r_x}{2} \delta_x (M_{i,j}^{k+1} + M_{i,j}^k) - \frac{r_y}{2} \delta_y (N_{i,j}^{k+1} + N_{i,j}^k). \end{aligned} \quad (2.32)$$

Equation (2.32) is the product of Δt and the local discretization error of the Crank-Nicolson scheme, that is

$$(\Delta t \tau_{i,j}^k)_{CN} = \Delta t \tau_{i,j}^k. \quad (2.33)$$

Repeat the same steps for corrector stage, from Eq.(2.5), we can formulate the local discretization error as follow

$$\begin{aligned} \Delta t \tau_{i+\frac{1}{2},j}^k &= \Delta t \left(M_t - \frac{v}{h} M_{xx} \right) \Big|_{i+\frac{1}{2},j}^k + \Delta t \left(gh \eta_x + \frac{\alpha_1}{12} gh \eta_{xxx} + \frac{\alpha_2}{12} gh \eta_{xyy} + \frac{\alpha_3}{4} gh \eta_{xtt} \right) \Big|_{i,j}^k \\ &\quad - \left(1 - \frac{v r_x}{h \Delta x} \delta_{xx} \right) M_{i+\frac{1}{2},j}^{k+\frac{1}{2}} + \left(1 + \frac{v r_x}{h \Delta x} \delta_{xx} \right) M_{i+\frac{1}{2},j}^k \end{aligned}$$

$$\begin{aligned}
 & - \left(gh \frac{r_x}{2} \delta_x + \frac{\alpha_1}{24} gh r_x \delta_{xxx} + \frac{\alpha_2}{24} gh r_x \delta_{xyy} + \frac{\alpha_3}{8} r_x gh \delta_{xtt} \right) (\eta_{i,j}^{k+1} + \eta_{i,j}^k) \\
 & + \frac{vr_x}{2h \Delta x} \delta_{xx} \left(M_{i+\frac{1}{2},j}^{k+\frac{1}{2}} - M_{i+\frac{1}{2},j}^k \right) \\
 & - \frac{1}{2} \left(gh \frac{r_x}{2} + \frac{\alpha_1}{24} gh r_x \delta_{xxx} + \frac{\alpha_2}{24} gh r_x \delta_{xyy} + \frac{\alpha_3}{8} r_x gh \delta_{xtt} \right) (\eta_{i,j}^{k+1} - \eta_{i,j}^k),
 \end{aligned} \tag{2.34}$$

where,

$$\begin{aligned}
 \delta_{xxx} &= \cdot_{i+2,j} - 3 \cdot_{i+1,j} + 3 \cdot_{i,j} - \cdot_{i-1,j}, \\
 \delta_{xtt} &= \left(\cdot_{i+1,j}^{k+1} - 2 \cdot_{i+1,j}^{k+\frac{1}{2}} + \cdot_{i+1,j}^k \right) - \left(\cdot_{i,j}^{k+1} - 2 \cdot_{i,j}^{k+\frac{1}{2}} + \cdot_{i,j}^k \right), \\
 \delta_{xyy} &= \left(\cdot_{i+1,j+1} - 2 \cdot_{i+1,j} + \cdot_{i+1,j-1} \right) - \left(\cdot_{i,j+1} - 2 \cdot_{i,j} + \cdot_{i,j-1} \right).
 \end{aligned} \tag{2.35}$$

Repeat the same steps for Eq (2.7), yields the local discretization error as follow

$$\begin{aligned}
 \Delta t \tau_{i,j+\frac{1}{2}}^k &= \Delta t \left(N_t - \frac{v}{h} N_{yy} \right) \Big|_{i,j+\frac{1}{2}}^k + \Delta t \left(gh \eta_y + \frac{\alpha_1}{12} gh \eta_{yyy} + \frac{\alpha_2}{12} gh \eta_{yxx} + \frac{\alpha_3}{4} gh \eta_{ytt} \right) \Big|_{i,j}^k \\
 & - \left(1 - \frac{vr_y}{h \Delta y} \delta_{yy} \right) N_{i,j+\frac{1}{2}}^{k+1} + \left(1 + \frac{vr_y}{h \Delta y} \delta_{yy} \right) N_{i,j+\frac{1}{2}}^k \\
 & - \left(gh \frac{r_y}{2} \delta_y + \frac{\alpha_1}{24} gh r_y \delta_{yyy} + \frac{\alpha_2}{24} gh r_y \delta_{yxx} + \frac{\alpha_3}{8} r_y gh \delta_{ytt} \right) (\eta_{i,j}^{k+1} + \eta_{i,j}^k) \\
 & + \frac{vr_y}{2h \Delta y} \delta_{yy} \left(N_{i,j+\frac{1}{2}}^{k+\frac{1}{2}} - N_{i,j+\frac{1}{2}}^k \right) \\
 & - \frac{1}{2} \left(gh \frac{r_y}{2} + \frac{\alpha_1}{24} gh r_y \delta_{yyy} + \frac{\alpha_2}{24} gh r_y \delta_{yxx} + \frac{\alpha_3}{8} r_y gh \delta_{ytt} \right) (\eta_{i,j}^{k+1} - \eta_{i,j}^k),
 \end{aligned} \tag{2.36}$$

where,

$$\delta_{yyy} = \cdot_{i,j+2} - 3 \cdot_{i,j+1} + 3 \cdot_{i,j} - \cdot_{i,j-1},$$

$$\delta_{ytt} := \left(\cdot_{i,j+1}^{k+1} - 2 \cdot_{i,j+1}^{k+\frac{1}{2}} + \cdot_{i,j+1}^k \right) - \left(\cdot_{i,j}^{k+1} - 2 \cdot_{i,j}^{k+\frac{1}{2}} + \cdot_{i,j}^k \right),$$

$$\delta_{yxx} := \left(\cdot_{i+1,j+1} - 2 \cdot_{i,j+1} + \cdot_{i-1,j+1} \right) - \left(\cdot_{i+1,j} - 2 \cdot_{i,j} + \cdot_{i-1,j} \right). \tag{2.37}$$

The first five terms at the right hand sides of Eqs. (2.34) and (2.36) are equal to zero but the last two terms remain such as they contain the numerical error of both linear dispersion and weakly dissipative.

A Taylor's series expansion would reveal that

$$\tau^k = \left(\tau_{i,j}^k \right)_{CN} + \tau_{i+\frac{1}{2},j}^k + \tau_{i,j+\frac{1}{2}}^k. \tag{2.38}$$

Expanding the remaining terms in a Taylor's series, yields

$$\begin{aligned} & \frac{\nu r_y}{2h \Delta y} \delta_{yy} \left(N_{i,j+\frac{1}{2}}^{k+\frac{1}{2}} - N_{i,j+\frac{1}{2}}^k \right) - \frac{1}{2} \left(gh \frac{r_y}{2} + \frac{\alpha_1}{24} gh r_y \delta_{yyy} + \frac{\alpha_2}{24} gh r_y \delta_{yxx} + \frac{\alpha_3}{8} r_y gh \delta_{ytt} \right) (\eta_{i,j}^{k+1} - \eta_{i,j}^k) \\ & = \frac{\nu r_y}{4h \Delta y} \Delta t \delta_{yy} \delta_t N_{i,j+\frac{1}{2}}^k - \frac{1}{2} \left(gh \frac{r_y}{2} \delta_y + \frac{\alpha_1}{24} gh r_y \delta_{yyy} + \frac{\alpha_2}{24} gh r_y \delta_{yxx} + \frac{\alpha_3}{8} r_y gh \delta_{ytt} \right) \Delta t \delta_t \eta_{i,j}^{k+\frac{1}{2}}. \end{aligned} \tag{2.39}$$

Thus, the local discretization error of the ADI method depends on the error of Crank-Nicolson scheme. From Eq. (2.39), when $\Delta t \rightarrow 0$, we get $\tau_{i+\frac{1}{2},j}^k$ (resp., $\tau_{i,j+\frac{1}{2}}^k$) $\rightarrow 0$. Then, the system of Eqs.(2.4) - (2.7) converges and has a truncated error given by

$$\tau^k = \left(\tau_{i,j}^k \right)_{CN} + (\Delta x)^3 + (\Delta x)(\Delta t)^2 + (\Delta x)^2(\Delta t). \tag{2.40}$$

3. Numerical Results and Discussion

The goal of this numerical study is recognition of mathematical aspect when nonlocal terms give a more realistic profile to dispersive free surface of tsunami. Surpass the obstacle that appears in the experimental when we introduce delicate values of ν , i.e., values of ν in nature. There are some time intervals for which the solution is Bichromatic Wave (BW). These intervals intersect only at the points $x \in [0, 15 \text{ m}]$, so that (BW) for this mode is established only at these values.

3.1 Free Surface Profile

Free surface elevation of (HTS1) propagation into ocean is well discussed in [16]. Following this application, our simulation focuses at waves dispersive affected by weak dissipation. (IWTs) propagation generated by tsunami source didn't discuss in the literature, for this we will explain the effects of ocean viscosity by virtue of

mathematical aspect. The choice of the kinematic viscosity for the practical simulations of water waves is not obvious. However, in various experimental and theoretical studies, researchers independently concluded that, a value of $\nu = 10^{-3} \text{ m}^2/\text{s}$ fits very well available data (see, [10]). The most recent experimental study of plunging breakers confirms this value again. Consequently, we retain this value for our numerical illustrations as well. Then, according to the criteria provided in [11] and satisfying Eq. (2.16), it is advisable to choose $B = 1/21$. Firstly, we study tendency of numerical solution convergence.

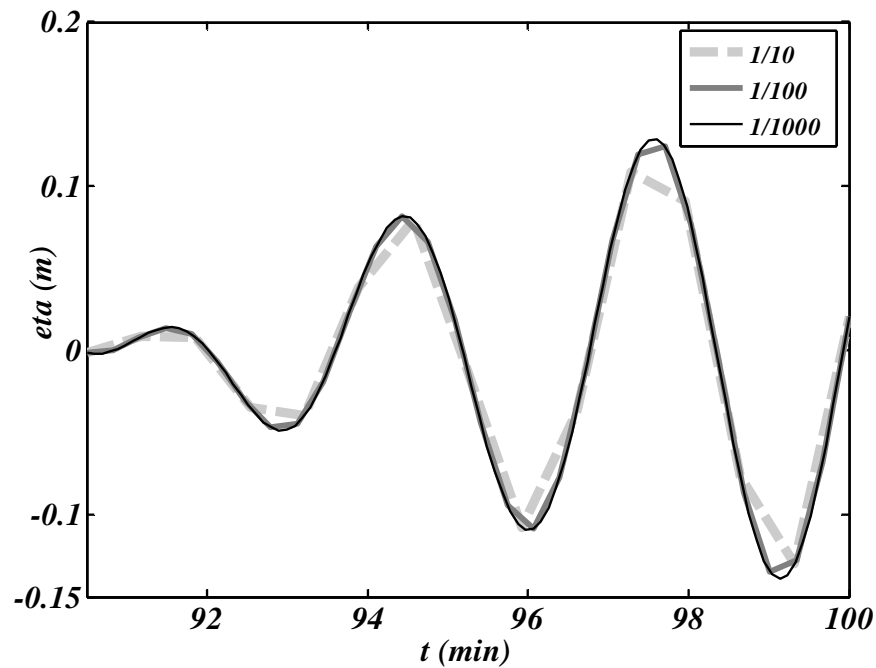


Figure 3. Free surface profile along with 6 mof the beginning dispersion for grid sizes: $\Delta x = \frac{1}{10}, \frac{1}{100}, \frac{1}{1000}$.

The relative error (rerr) is defined by following relationship:

$$\text{rerr} = \sqrt{\frac{\sum_{i=1}^{\lambda_x} \sum_{j=1}^{\lambda_y} [\eta(i,j) - \eta_{\text{ref}}(i,j)]^2}{\sum_{i=1}^{\lambda_x} \sum_{j=1}^{\lambda_y} [\eta_{\text{ref}}(i,j)]^2}}, \tag{3.1}$$

where, $\eta_{\text{ref}}(i,j)$ is calculated at $\Delta x = 1/1000$ as a reference among the proposed solutions.

Table 1. Relative error for refining proposed.

Time (min)	rerr of $\eta_{\frac{1}{10}}$	rerr of $\eta_{\frac{1}{100}}$
92	2.13457e - 02	1.34467e - 04
94	2.81415e - 02	1.77726e - 04
96	5.65162e - 01	3.56673e - 05
98	6.95978e - 01	4.36707e - 06
100	2.81622e - 03	1.76797e - 05

Figure 3 and Table 1, show that the error decreases gradually as Δx approaches zero. Then, the error between the approximate solution and the exact solution decreases corresponding to the theoretical convergence of order $O((\Delta x)^3, (\Delta x)(\Delta t)^2, (\Delta x)^2(\Delta t))$, (see section: Convergence of the Scheme).

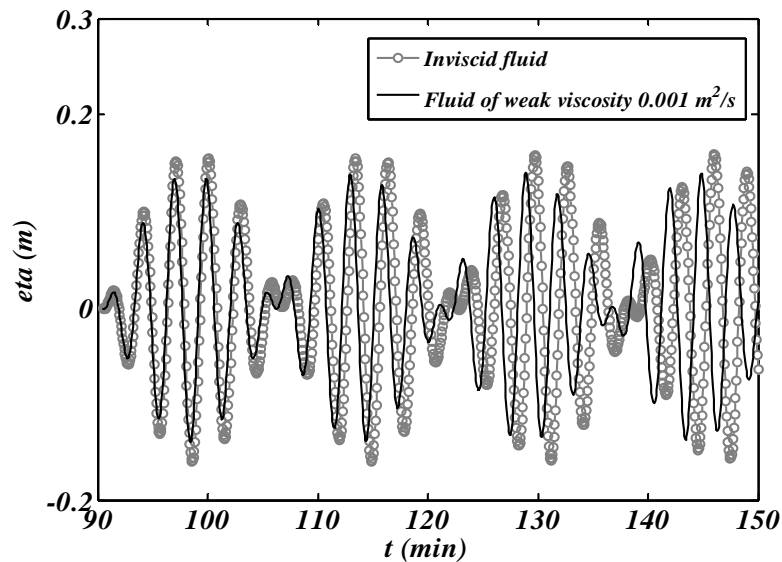


Figure 4.(BW) propagation in deep water with surface elevation 15 m from west boundary at

$$\Delta x = 0.001 \text{ m}, \Delta t = 4.16 \text{ sec}, h = 50 \text{ m}.$$

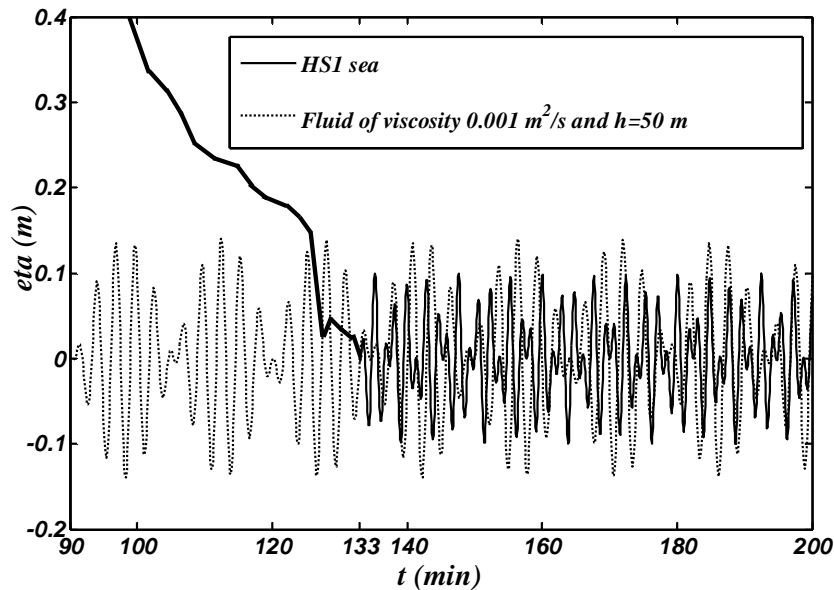


Figure 5. Comparison **(BW)** free surface profile between fluid of viscosity ($0.001 \text{ m}^2/\text{s}$) and **(HS1)** fluid.

(BW) propagates at 15 m and it travels down at an interval of time ******** $[90 \text{ min}, 150 \text{ min}]$ which almost undisturbed as shown in Figure 4. By using the same data for inviscid fluid which solved by (2.4)-(2.7) system with $\nu = 0 \text{ m}^2/\text{s}$. Figure 4 shows a clear decreased in train amplitudes for the viscous fluid compared to the inviscid. ******** Also, the wave propagation is slightly slow down by viscous effects. Mathematically this effect is ascribed to nonlocal terms which are more important in magnitude for small wave-numbers, ******** (see, [10]).

For comparison, the molecular viscosity of **(HTS1)** is of the order $\nu \approx 10^{-6} \text{ m}^2/\text{s}$ which is too small to model the energy dissipation phenomena in a laboratory wave tank. Hence, the molecular viscosity replaced in the Figures 3 and 4 by an effective value $10^{-3} \text{ m}^2/\text{s}$. We quote that **(BW)** begins to propagate after one hour and half of the initial free surface movement, but it appearing in Heraklion ocean site after two hour. Therefore, in the real problem, irregular wave has more than half an hour retard time comparing to fluid of $\nu = 10^{-3} \text{ m}^2/\text{s}$, see Figure 5.

3.2 Validation of the Numerical Scheme

Current method is validated against published numerical data in [11]. So, we compare our numerical results to the same it data, which investigated the propagation of **(IWTs)** over a constant water depth.

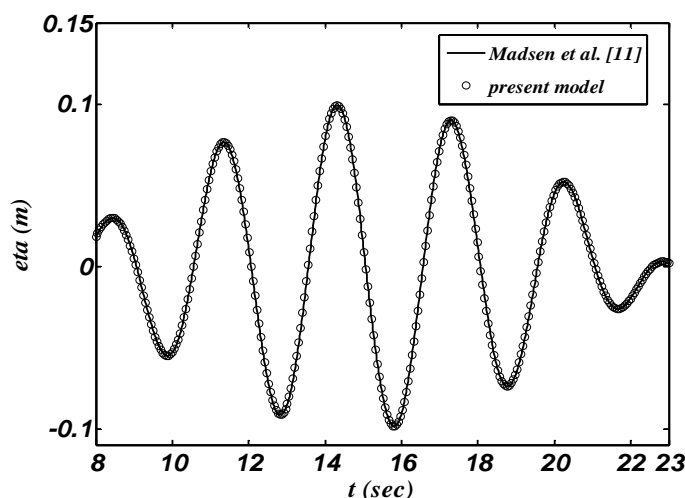


Figure 6. Comparison of (BW) free surface calculated using present finite difference method and the numerical scheme of [11] for the case $h = 4.2$ m.

Figure 6 shows a correlation between the work of [11] and our work. The use of [11] is performed with a uniform grid size of 0.6 m, it conducted into 12 m of channel. On the other hand, employing the present model (2.4)-(2.7) with $\nu = 0$ m²/s is made with a same grid size; but the time step Δt is determined from the stability criteria (2.17). The algorithms to compute various physical processes, such as nonlinear advection, nonlinear dispersion and wave dissipation due to bottom friction and breaking, are eliminated from the source scheme of the both [11] and (2.4)-(2.7) models. Thus, the computational time for the [11] model to calculate the free surface of (BW) can be measured for fair comparison with that of the present model. The numerical simulation is conducted for 90 sec after the initial water surface displacement imposed along $x = 0$ is released. The computational time elapsed for the two models are presented in Table 2. The [11] model employing a PC scheme consumes a long computational time, while the present fully implicit model takes about 1/10 of the computational time required for [11]. The computational efficiency of the present model can be realized even more dramatically if the computational time is compared with that of [11] of the best grid size of $\Delta x = 0.6$ m. The present model is approximately 10 times faster than the [11] model. It can be concluded that the present model is well efficient for practical problems.

Table 2. Comparison of computational time

Model	Madsen et al.[11]	Present modified scheme
Δx (m)	0.6	0.6
Number of grids	20×10	20×20
Δt (sec)	0.1	0.9
Number of time steps	14	7
CPU time (sec)	770	72

4. Conclusion

We have applied a novel scheme of dispersive propagation model for earthquake generated tsunami. It was also shown that simulations including both dispersive long distant tsunami propagation as well as weak dissipation are well achieved. As a benefit, our work can model the earthquake source flexibly in the propagation model. It is a useful numerical solution when existing theories are not available to find exact solution; this last is ideal and sometimes is not compatible with the physical phenomenon. Also experimental study is unable to achieve natural profile of solution because the inability to employ natural values.

In this model, we proposed the introducing an additional term to the novel modified scheme. This latter is comparatively has some limitations, i.e., the grid size has to be equal in both horizontal directions and check stability criteria (2.17). In other words, our approach calculates the dispersion-correction factors instead of choosing spatial grid size and step size again to mimic the frequency dispersion of the (ILBqs), [11]. The obtained numerical solutions are validated by [11] model. Remarkable results are more agreeable to our numerical model.

The relative danger of viscosity when its values decrease at greater temperatures which are due by Global Warming effect. Although the inverse temperature-viscosity relationship is a universal feature of aquatic systems, little mathematical research has been done to study the mathematical consequences of simultaneous changes in temperature and viscosity in (CLBqs). The effect of new viscous-temperature terms is to be revealed in futures studies. For inviscid case, we hope to solve Eq.(2.7) by numerical technique.

Appendix

$$A_x = \begin{bmatrix} 1 - a_3^x & 0 & 0 & 0 & \dots & 0 \\ -2a_3^x & 1 - a_3^x & 0 & 0 & \ddots & \vdots \\ a_3^x & -2a_3^x & 1 - a_3^x & 0 & \ddots & \vdots \\ 0 & a_3^x & -2a_3^x & 1 - a_3^x & \ddots & 0 \\ \vdots & \ddots & \backslash & \backslash & \backslash & \vdots \\ 0 & \dots & 0 & a_3^x & -2a_3^x & 1 - a_3^x \end{bmatrix}$$

$$E_x = \begin{bmatrix} 1 - cr_x & cr_x & 0 & \dots & 0 \\ 0 & 1 - cr_x & cr_x & \ddots & \vdots \\ \vdots & \ddots & 1 - cr_x & \backslash & 0 \\ \vdots & \ddots & \ddots & \backslash & cr_x \\ 0 & \dots & 0 & 0 & 1 - cr_x \end{bmatrix},$$

$$G_x = \begin{bmatrix} 1 & 0 & 0 & 0 & \dots & 0 \\ D_x & -F_x & 0 & 0 & \dots & \vdots \\ e_1^x & 0 & 0 & 0 & \dots & \vdots \\ e_2^x & e_3^x & -F_x & 0 & \dots & \vdots \\ 0 & 1 & 0 & 0 & \dots & \vdots \\ 0 & D_x & -F_x & 0 & \dots & \vdots \\ 0 & e_1^x & 0 & 0 & \ddots & \vdots \\ 0 & e_2^x & e_3^x & -F_x & \ddots & \vdots \\ \vdots & \dots & \ddots & \ddots & 0 & 1 & 0 & 0 & 0 & 0 \\ 0 & \dots & 0 & D_x & -F_x & 0 & 0 & 0 & 0 & 0 \\ & & & e_1^x & 0 & 0 & 0 & 0 & 0 & 0 \\ & & & e_2^x & e_3^x & -F_x & 0 & 0 & 0 & 0 \end{bmatrix},$$

$$K_x = \begin{bmatrix} 1 & 0 & 0 & 0 & \dots & 0 \\ D_x & 0 & 0 & 0 & \dots & \vdots \\ e_4^x & 0 & 0 & 0 & \dots & \vdots \\ e_5^x & e_6^x & 0 & 0 & \dots & \vdots \\ 0 & 1 & 0 & 0 & \dots & \vdots \\ 0 & D_x & 0 & 0 & \dots & \vdots \\ 0 & e_4^x & 0 & 0 & \ddots & \vdots \\ 0 & e_5^x & e_6^x & 0 & \ddots & \vdots \\ \vdots & \dots & \ddots & \ddots & 0 & 1 & 0 & 0 & 0 & 0 \\ 0 & \dots & 0 & D_x & 0 & 0 & 0 & 0 & 0 & 0 \\ & & & e_4^x & 0 & 0 & 0 & 0 & 0 & 0 \\ & & & e_5^x & e_6^x & 0 & 0 & 0 & 0 & 0 \end{bmatrix}, L_x$$

$$= \begin{bmatrix} 1 & 0 & 0 & 0 & \dots & 0 \\ D_x^* & 0 & 0 & 0 & \dots & \vdots \\ e_{10}^x & 1 & 0 & 0 & \dots & \vdots \\ e_{11}^x & e_{12}^x & 0 & 0 & \dots & \vdots \\ 0 & 1 & 0 & 0 & \dots & \vdots \\ 0 & D_x^* & 0 & 0 & \dots & \vdots \\ 0 & e_{10}^x & 1 & 0 & \dots & \vdots \\ 0 & e_{11}^x & e_{12}^x & 0 & \dots & \vdots \\ \vdots & \dots & \ddots & \ddots & 0 & 1 & 0 & 0 & 0 & 0 \\ 0 & \dots & 0 & D_x^* & 0 & 0 & 0 & 0 & 0 & 0 \\ & & & e_{10}^x & 1 & 0 & 0 & 0 & 0 & 0 \\ & & & e_{11}^x & e_{12}^x & 0 & 0 & 0 & 0 & 0 \end{bmatrix},$$

$$P_x = \begin{bmatrix} 1 & 0 & 0 & 0 & \dots & 0 \\ D_x^* & 0 & 0 & 0 & \dots & \vdots \\ e_7^x & 1 & 0 & 0 & \dots & \vdots \\ e_8^x & e_9^x & 0 & 0 & \dots & \vdots \\ 0 & 1 & 0 & 0 & \dots & \vdots \\ 0 & D_x^* & 0 & 0 & \dots & \vdots \\ 0 & e_7^x & 1 & 0 & \dots & \vdots \\ 0 & e_8^x & e_9^x & 0 & \dots & \vdots \\ \vdots & \vdots & \vdots & \vdots & \vdots & \vdots \\ 0 & \dots & 0 & 0 & 0 & 0 \end{bmatrix}, Q_x = \begin{bmatrix} 0 & 0 & 0 & 0 & \dots & 0 \\ 0 & 0 & 0 & 0 & \dots & \vdots \\ 1 & 0 & 0 & 0 & \dots & \vdots \\ 1 & F_x & 0 & 0 & \dots & \vdots \\ 0 & 0 & 0 & 0 & \dots & \vdots \\ 0 & 0 & 0 & 0 & \dots & \vdots \\ 0 & 1 & 0 & 0 & \dots & \vdots \\ 0 & 1 & F_x & 0 & \dots & \vdots \\ \vdots & \vdots & \vdots & \vdots & \vdots & \vdots \\ 0 & \dots & 0 & 1 & F_x & 0 \end{bmatrix}$$

$$S_x = \begin{bmatrix} -\frac{\alpha_3}{8} R_x Q_x & 0 & \dots & 0 \\ 0 & -\frac{\alpha_3}{8} R_x Q_x & \vdots & 0 \\ \vdots & \vdots & \backslash & -\frac{\alpha_3}{8} R_x Q_x \\ 0 & \dots & 0 & \dots \end{bmatrix}$$

$$U_x = \begin{bmatrix} a_1^x | & 0 & 0 & 0 & \dots & 0 \\ a_3^x | & a_1^x | & 0 & 0 & \dots & \vdots \\ a_3^x | & a_3^x | & a_1^x | & 0 & \dots & \vdots \\ 0 & a_3^x | & a_3^x | & a_1^x | & \dots & 0 \\ \vdots & \vdots & \backslash & \backslash & \backslash & \vdots \\ 0 & \dots & 0 & a_3^x | & a_3^x | & a_1^x | \end{bmatrix}, V_x = \begin{bmatrix} a_2^x | & 0 & 0 & \dots & 0 \\ -a_2^x | & a_2^x | & 0 & \dots & \vdots \\ 0 & -a_2^x | & a_2^x | & \dots & 0 \\ \vdots & \vdots & \backslash & \backslash & \vdots \\ 0 & \dots & 0 & -a_2^x | & a_2^x | \end{bmatrix}$$

$$W_x = \begin{bmatrix} \frac{\alpha_1}{8} R_x L_x & 0 & 0 & 0 & \dots & 0 \\ \alpha_2 R_x P_x & \frac{\alpha_1}{8} R_x L_x & 0 & 0 & \vdots & \vdots \\ \alpha_2 R_x K_x & \alpha_2 R_x P_x & \frac{\alpha_1}{8} R_x L_x & \frac{\alpha_1}{8} R_x L_x & \vdots & 0 \\ 0 & \alpha_2 R_x K_x & \alpha_2 R_x P_x & \alpha_2 R_x L_x & \vdots & 0 \\ \vdots & \vdots & \vdots & \vdots & \vdots & \vdots \\ 0 & \dots & 0 & \alpha_2 R_x K_x & \alpha_2 R_x P_x & \frac{\alpha_1}{8} R_x L_x \end{bmatrix},$$

$$Z_x = \begin{bmatrix} -\frac{\alpha_3}{8} R_x G_x & 0 & \dots & 0 \\ 0 & -\frac{\alpha_3}{8} R_x G_x & \vdots & 0 \\ \vdots & \vdots & \vdots & 0 \\ 0 & \dots & 0 & -\frac{\alpha_3}{8} R_x G_x \end{bmatrix},$$

$$F_x = \frac{1}{c r_x (1 - a_3^x)}, H_x = \frac{1 - c r_x}{c r_x (1 - a_3^x)}, \text{**** } D_x = a_3^x (H_x - c r_x F_x) - F_x, D_x^* = a_3^x (H_x - c r_x F_x) + F_x, R_x = \frac{g h r_x (\Delta x)^2}{(\Delta x)^2 + 2 v r_x}.$$

$$a_1^x = \frac{(\Delta x)^2 - 2 v r_x}{(\Delta x)^2 + 2 v r_x}, a_2^x = \frac{-r_x (\Delta x)^2}{24 [(\Delta x)^2 + 2 v r_x]}, a_3^x = \frac{v r_x}{(\Delta x)^2 + 2 v r_x}, e_1^x = (a_3^x - 1) [a_3^x (H_x - c r_x F_x) - F_x] + F_x,$$

$$e_2^x = [a_3^x (H_x - c r_x F_x) - F_x] [(a_3^x)^2 (H_x - c r_x F_x) - a_3^x + F_x] +$$

$$F_x [H_x + a_3^x (H_x - c r_x F_x)] - H_x.$$

$$e_3^x = F_x (1 - H_x + c r_x F_x),$$

$$e_4^x = a_3^x (H_x - c r_x F_x) [a_3^x (H_x - c r_x F_x) + F_x - 1] + F_x,$$

$$e_5^x = a_3^x (H_x - c r_x F_x) [a_3^x (H_x - c r_x F_x) + F_x - 1] + (H_x - c r_x F_x)$$

$$[a_3^x (H_x - c r_x F_x) + F_x] - H_x.$$

$$e_6^x = F_x [a_3^x (H_x - c r_x F_x) + H_x].$$

$$e_7^x = a_3^x (H_x - c r_x F_x) [a_3^x (H_x - c r_x F_x) + F_x - 1] + F_x + 2,$$

$$e_8^x = [a_3^x (H_x - c r_x F_x) + H_x] \{ a_3^x (H_x - c r_x F_x) [a_3^x (H_x - c r_x F_x) - 1] + F_x + 2 \}$$

$$[F_x + H_x (1 - a_3^x)] [a_3^x (H_x - c r_x F_x) + F_x] - H_x + F_x,$$

$$e_9^x = H_x + a_3^x (H_x - c r_x F_x) + 2 F_x.$$

$$e_{10}^x = a_3^x(H_x - cr_x F_x)[a_3^x(H_x - cr_x F_x) + F_x] - a_3^x(H_x - cr_x F_x) + F_x \\ - F_x(-2\alpha_1 + 24\alpha_2 + 3\alpha_3 + 6).$$

$$e_{11}^x = [H_x + a_3^x(H_x - cr_x F_x)]\{a_3^x[a_3^x(H_x - cr_x F_x) + F_x](H_x - cr_x F_x) + F_x \\ + (-2\alpha_1 + 24\alpha_2 + 3\alpha_3 + 6)[F_x + H_x(1 - a_3^x)][a_3^x(H_x - cr_x F_x) \\ + F_x] + H_x + F_x(-2\alpha_1 + 24\alpha_2 + 3\alpha_3 + 6)\},$$

$$e_{12}^x = -H_x - a_3^x(H_x - cr_x F_x) - F_x(-2\alpha_1 + 24\alpha_2 + 3\alpha_3 + 6).$$

Similarly, we can get the matrices and their coefficients according to y –direction; except the matrix S_x which is defined only for x –direction.

Acknowledgement

The* authors* would*like*to *thank *Prof.*Maurizio*Brocchini*from UniversitàPolitecnicadelle Marche, Department of Civil Engineering and Architecture (DICEA),***Italy, Ancona, for helpful discussions on viscous improved Boussinesq equations.

REFERENCES

- [1] Boussinesq, J.V., 1871, "Théorie générale des mouvements qui sont propagés dans un canal rectangulaire horizontal," *Comp. Rend. Hebd. des Seances de l'Acad. des Sci.*, 73, pp. 256–260.
- [2] Boussinesq, J.V., 1872, "Théorie des ondes et des remous qui se propagent le long d'un canal rectangulaire horizontal, en communiquant au liquide contenu dans ce canal des vitesses sensiblement pareilles de la surface au fond," *Journal de Mathématiques Pures et Appliquées*, 17, pp. 55–108.
- [3] Christov, C.I., and Choudhury, J., 2011, "Perturbation solution for the 2D Boussinesq equation," *Mech. Res. Comm.*, 38, pp. 274–28.
- [4] Daripa, P., and Hua, W., 1999, "A numerical study of an ill-posed Boussinesq equation arising in water waves and nonlinear lattices: Filtering and regularization techniques," *Appl. Math. Comput.*, 101, pp.159–207.
- [5] Bratsos, A.G., Tsitouras, Ch., and Natsis, D.G., 2005, "Linearized numerical schemes for the Boussinesq equation," *Appl. Num. Anal. Comp. Math.*, 2(1), pp. 34-53.
- [6] Antonopoulos, D.C., Dougalis, V.A., and Mitsotakis, D.E., 2010, "Numerical solution of Boussinesq systems of the Bona–Smith family," *Appl. Numer. Math.*, 60(4), pp.314-336.
- [7] Mitsotakis, D.E., 2009, "Boussinesq systems in two space dimensions over a variable bottom for the generation and propagation of tsunami waves," *Math. Comput. Simulation*, 80, pp.860–873.

- [8] Dougalis, V.A., Mitsotakis, D.E., and Saut, J.-C., 2007, "On some Boussinesq systems in two space dimensions: theory and numerical analysis," *ESAIM: Mathematical Modelling and Numerical Analysis*, 41(5), pp.825-854.
- [9] Antonopoulos, D.C., and Dougalis, V.A., 2012, "Numerical solution of the 'classical' Boussinesq system," *Math. Comput. Simulation*, 82, pp.984-1007.
- [10] Dutykh, D., and Goubet, O., "Derivation of dissipative Boussinesq equations using the Dirichlet-to-Neumann operator approach," *Math. Comput. Simulation*, in press.
- [11] Madsen, P.A., Murray, R., and Sørensen, O.R., 1991, "A new form of the Boussinesq equations with improved linear dispersion characteristics," *Coastal Eng.*, 15, pp.371-388.
- [12] Madsen, P.A., and Sørensen, O.R., 1992, "A new form of the Boussinesq equations with improved linear dispersion characteristics. Part 2. A slowly-varying bathymetry," *Coastal Eng.*, 18, pp.183-204.
- [13] Madsen, P.A., Fuhrman, D.R., and Schaffer, H.A., 2008, "On the solitary wave paradigm for tsunamis," *J. Geophys. Res.*, 113, C12012.
- [14] Yang, Z., Liu, S., Bingham, H.B., and Li, J., 2014, "Second-order coupling of numerical and physical wave tanks for 2D irregular waves. Part I: Formulation, implementation and numerical properties," *Coastal Eng.*, 92, pp. 48-60.
- [15] Koh, H.L., Teh, S.Y., Liu, P. L-F., Ismail, A. I. Md., and Lee, H.L., 2009, "Simulation of Andaman 2004 tsunami for assessing impact on Malaysia," *J. Asian Earth Sci.*, 36(1), pp. 74-83.
- [16] Flouri, E.T., Kalligeris, N., Alexandrakis, G., Kampanis, N.A., and Synolakis, C.E., 2013, "Application of a finite difference computational model to the simulation of earthquake generated tsunamis," *Appl. Numer. Math.*, 67, pp. 111-125.
- [17] Warming, R.F., and Hyett, B.J., 1974, "The modified equation approach to the stability and accuracy analysis of finite difference methods," *J. Comput. Phys.*, 14(2), pp.159-179.
- [18] Douglas Jr., J., and Gunn, J.E., 1964, "A General Formulation of Alternating Direction Methods, Part I, parabolic and hyperbolic problems," *Numer. Math.*, 6, pp.428-453.
- [19] Lapidus, L., and Pinder, G.F., 1982, "Numerical Solution of Partial Differential Equations in Science and Engineering," Wiley, New York.
- [20] Douglas Jr., J., and Rachford, H.H., 1956, "On the numerical solution of heat conduction problems in two and three space variables," *Trans. Am. Math. Soc.*, 82, pp.421-439.